Role of Spin Saturated and Unsaturated Interaction Potentials in Extended Thomas-Fermi Approach

A dissertation submitted

For partial fulfillment of the requirement for

The award of the degree of

Masters of Science in

Physics

Under the supervision of

Dr. Manoj K. Sharma

(Associate Professor)

Submitted by

Shivani Jain

(301104015)

School of Physics and Material Science

Thapar University,

(Formerly Thapar Institute of Engineering and Technology)

Patiala-147004, (Punjab) INDIA

July-2013

Dedicated To My

Respected

Parents

&

Teacher

Certificate

This is to certify that the thesis report entitled 'ROLE OF SPIN SATURATED AND UNSATURATED INTERACTION POTENTIALS IN EXTENDED THOMAS-FERMI APPROACH' submitted by **Ms. Shivani Jain** (Roll No. 301104015) of M.Sc. Physics, Thapar University, Patiala, was carried out by me under supervision and guidance **Dr. Manoj K. Sharma**. I have not submitted this material for credit towards any other degree at Thapar University, Patiala or any other university.

Date: 12th July 2013

Shivani Jain
(Shivani Jain)

12/7/13
Dr. Manoj K. Sharma
Associate Professor, SPMS
Thapar University,
Patiala.

Countersigned By:

Dr. Kulvir Singh
Head & Associate Prof.
SPMS, Thapar University,
Patiala.

Dr. S. K. Mohapatra
Dean of Academic Affairs
Thapar University,
Patiala.

Acknowledgement

First of all, I would like to thank **Dr. Manoj K. Sharma**, my worthy supervisor Associate professor School of Physics and Material Science, Thapar University, who has been an inspiration during my research work. Without him, this dissertation would not have been possible. I thank him for his patience and encouragement that carried me on through difficult times and for insight and suggestions that help to shape my research skills.

I also thank to **Dr. Kulvir Singh**, Professor and Head, School of Physics and Material Science for his support and providing facilities.

A special thank to **Ms. Deepika Jain**, research scholar for the help and valuable suggestions provided by her. Despite having a busy schedule she was always available for discussions and guidance. I am also thankful to my all classmates for their help and support during the course of this work. I owe my sincere gratitude to my family whose support and obstinate love gave me the energy to complete this dissertation work successfully and also for their untiring help during the difficult moment.

Shivani Jain

Shivani Jain

Abstract

The role of spin saturated and unsaturated interaction potentials have been studied in context of $^{23,25,27,29,31}Al + {}^{45}Sc \rightarrow {}^{68,70,72,74,76}Se^{*}$ reactions using semiclassical Extended Thomas-Fermi (ETF) approach in the framework of Skyrme Energy Density Formalism (SEDF) under frozen density approximation. Finally, the ℓ-summed extended Wong Model is used to investigate the fusion evaporation cross-sections of $^{27}Al + {}^{45}Sc$ reaction over a wide range of incident energies.

The present work consists of three chapters.

CHAPTER 1

Chapter1 contains the introductory part of spin saturated and unsaturated interaction potentials along with the knowledge of the nucleus-nucleus interactions. Besides this an emphasis is made on the module of semiclassical extended Thomas-Fermi approach and its possible use in the fusion evaporation and related phenomena.

CHAPTER 2

Chapter2 consists of the description of the ℓ-summed Extended Wong-Model. In this description I have explained the advantage of using different Skyrme forces like SIII and GSk1 via nuclear proximity potential which is calculated from SEDF. The relevant details regarding inclusion of deformation effects and penetration probability etc are duly incorporated in this chapter.

CHAPTER 3

Chapter3 consists of calculations and results. The calculations have been carried out for the spherical and deformed choice of nuclei in reference to the spin-orbit interaction potential for the isotopes of Al on fixed target ^{45}Sc using Skyrme forces SIII and GSk1. The fusion evaporation cross-sections are calculated in the framework of ℓ-summed Wong Model using Skyrme Energy Density Formalism (SEDF) approach for $^{27}Al + {}^{45}Sc$ reaction over a wide range of incident energies.

Contents

List of Figures

Chapter 3:

List of Tables

Chapter 3:

Chapter 1

Literature Review

Chapter 1

Introduction:

1.1 Nuclear Fusion Reaction

In Nuclear Physics, we study about the constituents and interactions of nuclei of the atoms. The interaction between the two nuclei gives rise to a nuclear reaction. Different kinds of nuclei in a nuclear reaction collide with each other, which in turn lead to a variety of compositions or decompositions of the nuclear systems. The formation of a new nucleus is generally associated with compound nucleus of the nuclear fusion reaction. The compound nucleus is an intermediate state in a nuclear fusion reaction in which the incident particle combine with the target nucleus and its energy is shared among all nucleons of the system. Once compound nucleus is formed depending on its mass, disintegrates by emitting multiple light particles (ER), followed by fission and the non-compound quasi-fission or deep inelastic collision process of a dinuclear system, where projectile and target are like fragments are seen in the decay channel. But here in our discussion, we focus on the fusion of two nuclei to understand the structure, stability, and the fusion cross-sections for a variety of nuclear systems.

In the nuclear fusion reaction, there are some factors which are generally considerable. The factors, which entail the nuclear fusion reaction, are masses, charges, deformations, orientations, degree of freedom and isospin. The interaction of symmetric reaction partners and asymmetric reaction partners has been of great interest in last few decades. It is so because masses and charges of interacting nuclei play very crucial role towards the formation and decay process of nuclear systems. Beside this the deformations and associated orientational features of nuclei involved are of extreme importance to investigate dynamics of nuclear reactions. In addition to this, the exchange symmetry between neutrons and protons is one of the most basic and fundamental principle of nuclear physics. It yields startling symmetries in the behavior of nuclei, and resulted in the introduction of isospin. Studies involving isospin effects have undergone resurgence in recent few years as such nuclei become more readily accessible.

The nuclear ion-ion interaction takes place because of the nature of the interacting nuclei. A well known aspect about the force between the charged nuclei is the repulsive Coulomb force plus an obscured short-ranged attractive force because of the exchange of the particles. The interaction causes a barrier between the two nuclei. The nuclear fusion reaction holds only when the projectile nucleus has enough energy to cross the Coulomb barrier. This information is essential for the understanding of nuclear phenomenon. A successful way of describing nuclear interaction is to construct one potential for the whole nucleus instead of considering all its nucleon constituents. This is called the macroscopic approach. In another way, a nuclear potential is suggested and an expression for the potential energy of two nuclear entities, either nuclei or nucleons, is developed. In order to estimate the parameters in this approach, some nucleon are added to a nucleus to investigate the effective role of additional nucleon. As one deal with

individual nucleons then the same is termed as microscopic approach for investigating nuclear behavior.

1.2 The Ion-Ion Interaction Potential

The ion-ion interaction potential of nuclei is mainly termed as total interaction potential. The total interaction potential is the sum of the Coulomb interaction, short-ranged nuclear interaction, and angular-momentum interaction potential. The total interaction potential can be represented by a simple expression

$$V(R) = V_C(R) + V_N(R) + V_\ell(R) \tag{1}$$

Where $V_C(R)$, is the repulsive Coulomb interaction potential, $V_N(R)$, is the attractive short-ranged nuclear interaction potential, and $V_\ell(R)$, is the angular-momentum interaction potential due to the orbital motion of the nucleus or nucleons.

It is well understood that the two terms of the total interaction potential i.e. the Coulomb interaction potential and the angular-momentum interaction potential are well defined that means a single approach is sufficient to define them. Unlikely, the nuclear interaction potential is not well-defined because of the unpredictable nature of the interaction involving variety of nuclei. As the nuclear interactions are short-ranged interactions, therefore the interaction is known as the proximity potential or nuclear proximity potential. The proximity interaction comes into picture when two nuclei approach each other within small distance ~ 2fm comparable to the surface thickness of interacting nuclei. The concept of the proximity potential is generated from the proximity theorem which was used for solving nuclear physics problems [1-3]. By using it, the nuclear potential, which is an important quantity for studying nuclear reaction and nuclear structure, can be easily determined. Many efforts have been put forward to give a simple and accurate form of the nuclear part of the ion-ion interaction potential [4-13]. The proximity model has been easily and successfully used to calculate the nuclear interaction between two nuclei. It is mainly composed of two parts. One depends on the shape and geometry of two nuclei, and other is the universal function only related to the short separation distance between two nuclei. Relating to the universal function, the proximity potential can be represented as given below

$$V_N^{prox77}(r) = 4\pi\gamma b\bar{R}\Phi(\xi) \tag{2}$$

Where $\bar{R}$ is the mean curvature radius and $\Phi(\xi)$ is the universal function, and the term γ can be given by the following expression

$$\gamma = \gamma_0\left[1 - k_s\left(\frac{N-Z}{A}\right)^2\right] \tag{3}$$

In the above expression, γ_o is the surface energy coefficient taken to be 0.9517 MeV/fm^2 for prox77. So, the isospin effects are studied by using various versions of the proximity potentials, since these potentials use the surface energy coefficient γ that depends on the isospin. The universal function, using the folding procedure, can also be calculated by using the Energy Density Function of Vautherin and Brink for the Skyrme force interactions [14]. Significant amount of work has been done [15-17] the direction using Energy Density Functional (EDF).

In the frame work of EDF, nuclear potential is calculated as a function of separation distance R as

$$V_N(R) = E(R) - E(\infty),$$

Where E represents the expectation value of colliding nuclei at overlapping distance R and at infinite distance. In this work we have used EDF based interaction potential as spin saturated and spin unsaturated terms can be independently worked out in this formulation. For the purpose we have adopted extended Thomas-Fermi approach details of which are discussed in this chapter and in chapter 2.

1.3 Skyrme Forces

The Skyrme force is an effective interaction depending on a limited number of parameters. The parameters of the Skyrme forces were fitted in literature [14, 18] to reproduce various bulk nuclear properties as well as selected properties of the normal and isospin-rich nuclei. The Skyrme force has six parameters t_o, t_1, t_2, t_3, x_o and W_o which has been adjusted by various authors time by time to get description of various ground state properties of nuclei. In the following expression, we can see the Skyrme force parameters in Hamiltonian density term as

$$\begin{aligned} H(\rho,\tau,J) = {} & \frac{\hbar^2}{2m}\tau + \frac{1}{2}t_0\left[\left(1+\frac{1}{2}x_o\right)\rho^2 - \left(x_0+\frac{1}{2}\right)\left(\rho_n^2+\rho_p^2\right)\right] + \frac{1}{12}t_3\rho^{\alpha_0}\left[\left(1+\frac{1}{2}x_3\right)\rho^2 - \left(x_3+\frac{1}{2}\right)\left(\rho_n^2+\rho_p^2\right)\right] \\ & + \frac{1}{4}\left[t_1\left(1+\frac{1}{2}x_1\right)+t_2\left(1+\frac{1}{2}x_2\right)\right]\rho\tau - \frac{1}{4}\left[t_1\left(x_1+\frac{1}{2}\right)-t_2\left(x_2+\frac{1}{2}\right)\right]\left(\rho_n\tau_n+\rho_p\tau_p\right) \\ & + \frac{1}{16}\left[3t_1\left(1+\frac{1}{2}x_1\right)-t_2\left(1+\frac{1}{2}x_2\right)\right]\left(\vec{\nabla}\rho\right)^2 - \frac{1}{16}\left[3t_1\left(x_1+\frac{1}{2}\right)-t_2\left(x_2+\frac{1}{2}\right)\right]\left[\left(\vec{\nabla}\rho_n\right)^2+\left(\vec{\nabla}\rho_p\right)^2\right] \\ & - \frac{1}{2}W_0\left(\rho\vec{\nabla}\vec{J}+\rho_n\vec{\nabla}\vec{J}_n+\rho_p\vec{\nabla}\vec{J}_p\right) \end{aligned} \tag{4}$$

Here, ρ_q, τ_q, and $\vec{J}$ (q=n, p) are the nucleonic, kinetic energy and spin-orbit densities, respectively. This Hamiltonian density equation is recently modified by Agrawal et al. [18]. In work of [18],

The third term in Eq. (4) is replaced as

$$\frac{1}{2}\sum_{i=1}^{3} t_{3i}\rho^{\alpha_i}\left[\left(1+\frac{1}{2}x_{3i}\right)\rho^2-\left(x_{3i}+\frac{1}{2}\right)\left(\rho_n^2+\rho_p^2\right)\right] \tag{5}$$

Beside this a new term due to tensor coupling with spin and gradient is added as

$$-\frac{1}{16}\left(t_1x_1+t_2x_2\right)\vec{J}^2+\frac{1}{16}\left(t_1-t_2\right)\left(\vec{J}_n^2+\vec{J}_p^2\right) \tag{6}$$

Recently [19], carried out a detailed analysis of some 240 Skyrme interaction parameter sets in order to justify the use of macroscopic properties of nuclear matter. In reference to current understanding some 16 Skyrme interactions were singled out. Here, we use one new force out of the 16 Skyrme interactions i.e. GSk1 which having stronger isospin and mass asymmetric effects and one old force i.e. SIII which having lesser isospin effect. It is relevant to mention here that the Skyrme's interactions can be described as a kind of phenomenological G matrix which influences the effects of the short-range correlations, notably through the density-dependent term. Skyrme's interaction is an approximate representation of the effective nucleon force which is only valid for low relative momenta.

The different parameterizations of the Skyrme force's parameters are termed by labeling them as S, SII, SIII, GSk1, GSk2 [18] etc. And the Skyrme force SIII is widely used to study the heavy-ion potential barriers at low energy.

1.4 Thomas-Fermi Model

Thomas-Fermi model is a quantum mechanical theory for the electronic structure of many-body systems developed semi-classically shortly after the introduction of the Schrodinger's equation. The brief description of using this model can be explained in a very simple ways. In recent years some of the Thomas-Fermi (TF) related theories for the ground states of non-relativistic atoms and molecules with fixed nuclei have been established in a mathematically rigorous way. The TF model's theory yields the collision between heavy-ion nuclei; there is huge number of nucleons in which the excitation energy is equilibrized amongst the nucleons. These excitations between the nucleons raise the concept of thermo-dynamical-statistical and then, excitation can be expressed in terms of an intrinsic temperature. These nuclei are also named as 'hot nuclei', produced as compound systems in energetic heavy-ion collisions. The formation of hot nuclei can play a crucial role for the formation of the star during the gravitational collapse of massive stars.

In isolated hot compound nuclei which are created in heavy-ion collisions, phase transitions don't strictly exist due to their finiteness. It is difficult to analyze the theoretical descriptions of the compound nucleus due to lack of an equilibrium situation. This lead to many variational calculations within static mean-field or Hartree-Fock theory, together with the use of suitable boundary conditions. It might be sufficiently well justified procedure for the description of the hot, metastable nuclei. This is to be noted, in the microscopic descriptions of such a system for T $\geq$ 3MeV, the shell effects are washed out and all the expectation values becomes smooth functions of particle numbers and deformation. In this case a semiclassical treatment in terms of densities and average fields is not only sufficient, but also much more economic and physically transparent. Semiclassical variational calculations for average ground-state properties and deformation energies of nuclei at T=0 have recently become very successful, particularly in connection with Skyrme-type effective interaction. Technically most refined of these semiclassical methods is the density variational method using local density functional for the kinetic energy and spin densities in a gradient expansion, derived from the so-called Thomas-Fermi model.

1.5 Energy Density Formalism (EDF)

Eventually, the Hartree-Fock method was applied as the microscopic background to build up the Energy Density Formalism (EDF). But under the sudden density approximation, the full HF calculations could not be applied in energy density formalism, due to lessly defined kinetic energy density τ of the compound nucleus at HF level. To overcome this difficulty, the semiclassical approaches to this quantity based on the Thomas-Fermi (TF) method or its extension that is Extended Thomas-Fermi (ETF) have been used for obtaining τ in the compound system. The kinetic energy density is obtained as a function of the local density ρ, for the spin independent potential in the power of $\hbar^2$ of the density matrix. In case of isolated nucleus, the ground state density is found from the energy density by a variational approach. It has been shown that the models based on macroscopic approach, like the liquid-drop model and Extended Thomas-Fermi model are able to reproduce the fusion data correctly. Therefore, out of a large number of available interaction potentials, the energy density formalism in semiclassical ETF approach has been used [20-22] which provides a convenient basis for the calculation of the interaction potential between the two colliding nuclei.

In EDF, the nucleus-nucleus interaction potential, as a function of separation distance, is defined as the difference of the energy expectation value of the colliding nuclei that are overlapping (at a finite separation distance R) and are completely separated ($R = \infty$) [23].The introduction of proximity potential in the form of an universal function, first for Thomas-Fermi nuclear densities and next for two parameter Fermi densities. The universality of such a universal function was later by Gupta and collaborators [24] and simple analytical expressions were given to represent the universal function of proximity potential. These functional forms could be worked out for spin-saturated nuclei or, equivalently, the spin-orbit density independent part of the interaction

potential $V_P(R)$ only, since the spin-orbit density dependent interaction potential $V_J(R)$ in this formalism depends on the filling of the shell model states and hence only a simple analytical functional form of $V_J(R)$ has been possible [17, 25].

In our discussion, it is of interest to obtain barrier heights and positions using the Skyrme energy density functional (SEDF). The Energy Density Functional used for the Skyrme interactions in which the Hamiltonian density is the function of the nucleon density, kinetic energy density, and the spin-orbit density.

The main stress is to understand the role of the spin-orbit density contribution to the nucleus-nucleus interaction potential [24, 26-30]. Consequently, the spin-orbit density part of the interaction potential can contribute towards the fusion barriers. The spin-orbit density part of the nucleus-nucleus interaction potential is, based on the Skyrme Energy Density Formalism (SEDF), expressed by two different approaches. In the one approach, the shell and structural effects are present (microscopic approach) in Hamiltonian and another one, no shell effect are present in Hamiltonian (semiclassical approach).

The semiclassical formulation of the Skyrme Energy Density Functional (SEDF) for spin-orbit density part of the interaction potential is compared with the microscopic shell model formulation [31]. The comparison yields same result for both the approaches. The motive of the comparison is to found out the easy calculations of the Skyrme Energy Density Functional for spin-orbit density part of the interaction potential.

It is relevant to mention here that, the semiclassical calculations are supposed to contain no shell effects whereas the microscopic calculations are lengthy because of inclusion of shell and structural effects [21]. In another way, the semiclassical calculations can reduce the lengthy process, and consequently the calculations are worked out in the frame-work of extended Thomas-Fermi model [20], which expresses the kinetic energy density τ and spin-orbit density $\vec{J}$ as functions of the nucleon density $\rho(\vec{r})$ [20, 21, 32, 33]. Thus, the Skyrme energy density becomes a function of the nucleon densities alone. The extended Thomas-Fermi model is used not only to give a very precise description of average nuclear properties but also reproduce some local quantities of neutron and proton densities, the corresponding potentials and spin-orbit potentials.

In Semiclassical microscopic approach, there are some assumptions, which are explained as follows:

Adiabatic Approximation

i. The approximation under which the time of collision being so slow that at each stage of the collision the nucleons of the two nuclear ions reach the equilibrium configuration, called the 'adiabatic approximation'.

Sudden Approximation

ii. The approximation under which the time of collision is so small that the internal structure of the two ions is unmodified and the nuclear density overlap without changing their shapes, called 'sudden density approximation' that includes the effect of exchange terms due to anti-symmetrization. The sudden density approximation excluding the effect of exchange terms is also known as frozen density approximation [34].

In our calculations we have used frozen density approximation to investigate the role of spin saturated and spin unsaturated interaction potentials in the framework of extended Thomas-Fermi approach. Semiclassical expansions derived in the framework of the Extended Thomas-Fermi approach for the spin-orbit density $J(r)$ and the kinetic energy density $\tau(\rho_q)$ as functions of the local density $\rho(r)$ are used to determine the nuclear potential distribution. Further details are discussed in Chapter 2.

Here, we are studying the role of the spin-orbit density part of the interaction potential in the semiclassical extended Thomas-Fermi (ETF) approach using Skyrme Energy Density Formalism (SEDF) under the frozen density approximation. From the assumptions of the semiclassical approach, it is well known that there are different forms of nucleon densities distributions i.e. sudden and frozen density approximations. These two approximations give us a unique possibility of analyzing the role of different density distributions. Sudden density approximation contains the exchange term i.e. exchange effects arise for the composite system whereas frozen density approximation has no such effects in which sum of the densities of two incoming nuclei as taken into account. The effect due to these approximations in the fusion barrier and fusion cross-section is seen [35]. The frozen density approximation gives more realistic barriers as compared to the sudden density approximation. Hence, the frozen density approximation in semiclassical ETF method based on SEDF seems to describe the fusion cross-section without involving barrier modification effects.

As nuclear proximity potential is discussed in two different distinct terms known as spin saturated (spin-orbit density independent) and unsaturated (spin-orbit density dependent) interaction potentials so the same are discussed below.

1.6 Spin Saturated and Unsaturated Interaction Potentials

The spin saturated and unsaturated interaction potentials behave oppositely from one another. The spin-orbit density dependent potential is repulsive and in the contrary, the spin-orbit density independent potential is attractive. In general, the spin unsaturated interaction potential has both the repulsive at large distances and attractive nature at smaller distances under the sudden approximation. But in case of the frozen approximation, only repulsive behavior is left due to no exchange effects in the sum of densities of nucleons. Also, when the spin-orbit density dependent potential changes its nature from repulsive to attractive it tends to zero [36]. Another term, the spin saturated potential, remains attractive at large distances and repulsive at smaller distances under both the frozen and sudden approximations. The sums of these potentials gives rise to nuclear interaction potential. In the present work, we calculate spin saturated and spin unsaturated interaction potential under frozen approximation rather than sudden approximation. This is due to reason that the barrier characteristics which are the main ingredient in calculating fusion excitation function within the frame work of ℓ-summed Wong model using SEDF approach is clearly observed [37] in frozen approximation.

An apparent need is to obtain a general analytical formula of the potential for both the spin saturated and unsaturated interaction potentials. Spin saturated potential depends on nucleon and kinetic energy densities and the spin unsaturated potential depends on the nucleon and spin densities. It may be interesting to know that the ion-ion interaction and the nuclear interaction potentials are the function of the deformations and orientations of the interacting nuclei, and can be represented as

$$V_T^{\ell}\left(R, E_{c.m.}, \theta_i\right) = V_C\left(R, Z_i, \beta_{\lambda i}, T, \theta_i\right) + V_N\left(R, A_i, \beta_{\lambda i}, T, \theta_i\right) + V_{\ell}\left(R, A_i, \beta_{\lambda i}, T, \theta_i\right)$$

With the inclusion of deformation and orientation effects of the colliding nuclei, the spin unsaturated interaction potential leads to the increase in the barrier height. Whereas, spin saturated potential lead to decrease in the barrier height. Hence, the sum of these two potentials gives rise to decrease in barrier height of the nuclear interaction potential with the inclusion of deformation and orientation. This means that the deformations affect the barrier positions significantly. Hence, the structure and orientation of the nucleus also influences the fusion cross-sections. Therefore nucleons of such effects are of extreme importance to analyze the dynamical features of heavy-ion reactions.

In summary, the contribution of the spin dependency/independency, separation distance, and deformations and orientations etc impart useful information regarding overall behavior of a nuclear system under investigation.

Proposed Work:

The Role of The Spin Saturated and Spin Unsaturated Interaction Potentials in $^{23,25,27,29,31}Al + ^{45}Sc \rightarrow ^{68,70,72,74,76}Se^{*}$ Reaction

We intent to investigate the spin saturated and spin unsaturated interaction potentials in context of $^{23,25,27,29,31}Al + ^{45}Sc \rightarrow ^{68,70,72,74,76}Se^{*}$ reactions. Main aim here to address the possible role of temperature and nuclear deformations in spin dependent and spin independent interaction potentials for above mentioned reactions. The possible role of the proximity potential (the sum of the spin saturated and spin unsaturated interaction potentials) obtained using semiclassical extended Thomas-Fermi approach, will be analyzed in reference to fusion cross-sections of $^{27}Al + ^{45}Sc$ reaction at near barrier energies using ℓ-summed extended Wong Model [38].

References:

[1] J. Blocki, J. Randrup, W.J. Swiatecki, C.F. Tsang, Ann. Phys. (NY) 105, 427(1977)

[2] W.D. Myers, W.J. Swiatecki, Phys. Rev. C 62, 044610(2000)

[3] P. M¨oller, J.R. Nix, Nucl. Phys. A 361, 117(1981)

[4] I. Dutt and R. K. Puri, Phys. Rev. C81, 044615(2010)

[5] I. Dutt and R. K. Puri, Phys. Rev. C81, 064609(2010)

[6] I. Dutt and R. K. Puri, Phys. Rev. C81, 047601(2010); I. Dutt and R. Bansal, Chin. Phys. Lett. 27, 112402(2010)

[7] R. K. Puri et al, Eur. Phys. J. A23, 429(2005); R. Arora et al, ibid. 8, 103(2000); R. K. Puri et al, ibid. 3, 277(1998); N. K. Dhiman et al, Acta. Phys. Pol. B38, 2133(2007); 37, 1855 (2006); I. Dutt and N. K. Dhiman, Chin. Phys. Lett. 27, 112401(2010)

[8] R. K. Gupta et al, Phys. Rev. C47, 561(1993); J. Phys. G: Nucl. Part. Phys. 18, 1533(1992); S. S. Malik et al., Pramana, J. Phys. G: 32, 419(1989); R. K. Puri et al., Eur. phys. Lett. 9, 767 (1989); J. Phys. G: Nucl. Part. Phys. 18, 903(1992)

[9] J. Blocki and W. J. Swia, tecki, Ann. Phys. (N.Y.) 132, 53(1981)

[10] W. Reisdorf, J. Phys. G: Nucl. Part. Phys. 20, 1297(1994)

[11] K. Siwek Wilczynska and J. Wilczy ´ nski, ´ Phys. Rev. C69, 024611(2004)

[12] M. Liu et al., Nucl. Phys. A768, 80(2006); A. Dobrowolski et al., ibid. 729, 713(2003); J. Bartel et al., Eur. Phys. J. A14, 179(2002)

[13] V. Y. Denisov, Phys. Lett. B526, 315(2002); V. Y. Denisov and V. A. Nesterov, Phys. At. Nucl. 69, 1472(2006)

[14] D. Vautherin and D. M. Brink, Phys. Rev. C3, 626(1972)

[15] C. Ngo et al., Nucl. Phys. A252, 237(1975)

[16] H. Ngo and C. Ngo, Nucl. Phys. A348, 140(1980)

[17] R. K. Puri and R. K. Gupta, Int. J. Mod. Phys. E1, 269(1992)

[18] B. K. Agrawal, S. K. Dhiman, and R. Kumar, Phys. Rev. C73, 034319(2006)

[19] M. Dutra et al., Phys. Rev. C 85, 035201(2012)

[20] M. Brack, C. Guet, and H. B. Hakansson, Phys. Rep. 123, 275(1985)

[21] J. Bartel and K. Bencheikh, Eur. Phys. J. A14, 179(2002).

[22] K. A. Brueckner, C. A. Levinson, and H. H. Mohmoud, Phys. Rev. 95, 217(1954)

[23] D. M. Brink and Fl. Stancu, Nucl. Phys. A270, 236(1976)

[24] R. K. Puri, P. Chattopadhyay, and R. K. Gupta, Phys. Rev. C43, 315(1991)

[25] M. K. Sharma, R. K. Puri, and R. K. Gupta, Eur. Phys. J. A2, 69(1998)

[26] K. C. Panda, J. Phys. G11, 1323(1985); K. C. Panda and T. Patra, ibdi. 14, 1489(1988)

[27] S. Kaur and P. Chattopadhyay, Phys. Rev. C36, 1016(1987)

[28] Li Guo-Qiang and Xu Gong-Ou, Nucl. Phys. A492, 340(1989)

[29] R. K. Puri and R. K. Gupta, Phys. Rev. C51, 1568(1995)

[30] R. K. Puri and R. K. Gupta, Phys. Rev. C45, 1837(1992)

[31] R. K. Gupta, D. Singh, and W. Greiner, Phys. Rev. C75, 024603(2007)

[32] B. Grammoticos and A. Voros, Ann. Phys. 123, 359(1979)

[33] B. Grammoticos and A. Voros, Ann. Phys. (NY) 129, 153(1980)

[34] G. Q. Li, J. Phys. G: Nucl. Part. Phys. 17, 1(1991)

[35] R. Kumar, R. K. Gupta, Intern. Symp. On Nucl. Phys., DAE, Mumbai, Dec. 8-12(2009)

[36] R. K. Gupta, D. Singh, R. Kumar, and W. Greiner, J. Phys. G: Nucl. Part. Phys. 36(2009) 075104 (11pp)

[37] R. Kumar, M. K. Sharma, and R. K. Gupta, Nucl. Phys. A870, 42-57(2011)

[38] C. Y. Wong, Phys. Rev. Lett. 31, 766(1973)

Chapter 2

Skyrme Energy Density Formalism (SEDF) & ℓ-summed Extended Wong Model

Chapter 2

2.1 The Skyrme Energy Density Formalism in Semiclassical Extended Thomas-Fermi (ETF) Method

The energy density formalism defines the nuclear interaction potential as

$$V_N(R) = E(R) - E(\infty) \tag{1}$$

i.e. the nucleus-nucleus interaction potential as a function of separation distance, $V_N(R)$ is the difference of the energy expectation value E of the colliding nuclei that are overlapping (at a finite separation distance R) and are completely separated (at $R=\infty$), where

$$E = \int H(\vec{r})d\vec{r} \tag{2}$$

With the Skyrme approach, the modified Hamiltonian in reference to [1] reaches as

$$\begin{aligned} H(\rho,\tau,J) = {} & \frac{\hbar^2}{2m}\tau + \frac{1}{2}t_0\left[\left(1+\frac{1}{2}x_o\right)\rho^2 - \left(x_0+\frac{1}{2}\right)\left(\rho_n^2+\rho_p^2\right)\right] + \frac{1}{2}\sum_{i=1}^{3}t_{3i}\rho^{\alpha_i}\left[\left(1+\frac{1}{2}x_{3i}\right)\rho^2 - \left(x_{3i}+\frac{1}{2}\right)\left(\rho_n^2+\rho_p^2\right)\right] \\ & + \frac{1}{4}\left[t_1\left(1+\frac{1}{2}x_1\right)+t_2\left(1+\frac{1}{2}x_2\right)\right]\rho\tau - \frac{1}{4}\left[t_1\left(x_1+\frac{1}{2}\right)-t_2\left(x_2+\frac{1}{2}\right)\right]\left(\rho_n\tau_n+\rho_p\tau_p\right) \\ & + \frac{1}{16}\left[3t_1\left(1+\frac{1}{2}x_1\right)-t_2\left(1+\frac{1}{2}x_2\right)\right]\left(\vec{\nabla}\rho\right)^2 - \frac{1}{16}\left[3t_1\left(x_1+\frac{1}{2}\right)-t_2\left(x_2+\frac{1}{2}\right)\right]\left[\left(\vec{\nabla}\rho_n\right)^2+\left(\vec{\nabla}\rho_p\right)^2\right] \\ & - \frac{1}{2}W_0\left(\rho\vec{\nabla}\vec{J}+\rho_n\vec{\nabla}\vec{J}_n+\rho_p\vec{\nabla}\vec{J}_p\right) - A\left[\frac{1}{16}\left(t_1x_1+t_2x_2\right)\vec{J}^2 - \frac{1}{16}\left(t_1-t_2\right)\left(\vec{J}_n^2+\vec{J}_p^2\right)\right] \end{aligned} \tag{3}$$

Here, $\rho = \rho_n + \rho_p$, $\tau = \tau_n + \tau_p$, and $\vec{J} = \vec{J}_n + \vec{J}_p$ are the nuclear, kinetic energy, and spin-orbit densities, respectively. m is the nucleon mass, and x_j, t_j (j=0, 1, 2), x_{3i}, t_{3i}, α_i, (i=1, 2, 3), W_0, and A are the Skyrme force parameters, fitted recently by Agrawal et al. [1], denoted GSk1, GSk2, and SSk forces. These authors modified the earlier well known [2, 3] Hamiltonian density by introducing six additional parameters in the third term [two each of x_{3i}, t_{3i}, and α_i (i=1, 2)], and an additional last term with constant A = 1 to account for tensor coupling with spin and gradient. For the other earlier fitted Skyrme forces [2, 3], such as SIII, SV, SkM*, etc., the constants A, x_{3i}, t_{3i}, and α_i (i=2, 3), are all zero, and $t_{31} = \frac{1}{6}t_3$, $x_{31} = x_3$, and $\alpha_1 = \alpha$.

The kinetic energy density in ETF method, taken up to second order terms for reasons of being enough for numerical convergence is (q = n or p)

$$\tau_q(\vec{r}) = \frac{3}{5}\left(3\pi^2\right)^{2/3}\rho_q^{5/3} + \frac{1}{36}\frac{\left(\vec{\nabla}\rho_q\right)^2}{\rho_q} + \frac{1}{3}\Delta\rho_q + \frac{1}{6}\frac{\vec{\nabla}\rho_q\cdot\vec{\nabla}f_q + \rho_q\Delta f_q}{f_q} - \frac{1}{12}\rho_q\left(\frac{\vec{\nabla}f_q}{f_q}\right)^2 +$$

$$\frac{1}{2}\rho_q\left(\frac{2m}{\hbar^2}\right)^2\left(\frac{\omega_0}{2}\frac{\vec{\nabla}\left(\rho+\rho_q\right)}{f_q}\right)^2 \qquad (4)$$

With f_q as the effective parameter mass form factor,

$$f_q(\vec{r}) = 1 + \frac{2m}{\hbar^2}\frac{1}{4}\left\{t_1\left(1+\frac{x_1}{2}\right) + t_2\left(1+\frac{x_2}{2}\right)\right\}\rho_q(\vec{r}) - \frac{2m}{\hbar^2}\frac{1}{4}\left\{t_1\left(x_1+\frac{1}{2}\right) - t_2\left(x_2+\frac{1}{2}\right)\right\}\rho_q(\vec{r}) \qquad (5)$$

The spin $\vec{J}$ is a purely quantal property, and hence has no contribution in the lowest (TF) order.

However, at the ETF level, the second order contribution gives

$$\vec{J}_q(\vec{r}) = -\frac{2m}{\hbar^2}\frac{1}{2}\omega_0\frac{1}{f_q}\rho_q\vec{\nabla}\left(\rho+\rho_q\right) \qquad (6)$$

Also, a function ρ_q or ρ alone. For the composite system, $\rho = \rho_1+\rho_2$

For sudden approximation,

$$\tau(\rho) = \tau(\rho_{1n}+\rho_{2n}) + \tau(\rho_{1p}+\rho_{2p})$$

$$\vec{J}(\rho) = \vec{J}(\rho_{1n}+\rho_{2n}) + \vec{J}(\rho_{1p}+\rho_{2p}) \qquad (7)$$

For frozen approximation,

$$\tau(\rho) = \tau(\rho_1) + \tau(\rho_2)$$

$$\vec{J}(\rho) = \vec{J}(\rho_1) + \vec{J}(\rho_2) \qquad (8)$$

With $\rho_i = \rho_{in}+\rho_{i}$,, $\tau_i(\rho_i) = \tau_{in}(\rho_{in})+\tau_{ip}(\rho_{ip})$, and $\vec{J}_i(\rho_i) = \vec{J}_{in}(\rho_{in}) + \vec{J}_{ip}(\rho_{ip})$.

Introducing slab approximation of semi-infinite nuclear matter with surfaces parallel to *x-y* plane, moving in *z*-direction, and separated by distance *s* having minimum value s_o, the interaction potential $V_N(R)$ between two nuclei separated by $R=R_1+R_2+s$ is given as,

$$\begin{aligned} V_N(R) &= 2\pi\bar{R}\int_{s_0}^{\infty} e(s)ds \\ &= 2\pi\bar{R}\int\left\{H(\rho,\tau,\vec{J})-\left[H_1(\rho_1,\tau_1,\vec{J}_1)+H_2(\rho_2,\tau_2,\vec{J}_2)\right]\right\}dZ \\ &= 2\pi\bar{R}\int\left\{\left(H(\rho)-\left[H_1(\rho_1)+H_2(\rho_2)\right]\right)+\left(H(\vec{J})-\left[H_1(\vec{J}_1)+H_2(\vec{J}_2)\right]\right)\right\}dZ \\ &= V_P(R)+V_J(R) \end{aligned} \tag{9}$$

Where $V_P(R)$ and $V_J(R)$ are the spin-density independent and spin-density dependent parts of the interaction potential; $\bar{R} = R_1+R_2/(R_1+R_2)$ is the mean curvature radius defining the geometry of the system.

For nuclear density ρ_i, we use the *T*-dependent Fermi density distribution

$$\rho_i(Z_i) = \rho_{0i}(T)\left[1+\exp\left(\frac{Z_i - R_i(T)}{a_i(T)}\right)\right]^{-1} \tag{10}$$

With $Z_2 = R - Z_1 = [R_1(\alpha_1)+R_2(\alpha_2)+s] - Z_1$, and central density

$$\rho_{0i}(T) = \frac{3A_i}{4\pi R_i^3(T)}\left[1+\frac{\pi^2 a_i^2(T)}{R_i^3(T)}\right]^{-1} \tag{11}$$

With nucleon densities ρ_{iq} further defined as

$$\rho_{in} = \frac{N_i}{A_i}\rho_i, \rho_{ip} = \frac{Z_i}{A_i}\rho_i$$

And the half density radii $R_{0i}(T=0)$ and the surface thickness parameters a_i (T=0) obtained by fitting the experimental data to polynomials in nuclear mass A (=4-209), as [4]

$$R_{0i}(T=0) = 0.90106\_0.10957A_i - 0.0013A_i^2 + 7.71458\times10^{-6}A_i^3 - 1.62164\times10^{-8}A_i^4,$$
$$a_i(T=0) = 0.34175 + 0.01234A_i - 2.1864\times10^{-4}A_i^2 + 1.46388\times10^{-6}A_i^3 - 3.24263\times10^{-9}A_i^4$$

(12)

The temperature dependence in the above formulae are then introduced as in Ref. [5]

$$R_{0i}(T) = R_{0i}(T=0)\left[1 + 0.0005T^2\right], a_i(T) = a_i(T=0)\left[1 + 0.01T^2\right] \quad (13)$$

Also, the surface width *b* is made *T* –dependent [6],

$$b(T) = 0.99\left(1 + 0.009T^2\right),$$

Where *T* is related to the incoming center-of-mass energy $E_{c.m.}$ or the compound nucleus (CN) excitation energy E^*_{CN} via the entrance channel Q_{in} -value, as

$$E^*_{CN} = E_{c.m.} + Q_{in} = \frac{1}{a}AT^2 - T \quad (14)$$

With a = 9 or 10, respectively, for intermediate mass or superheavy systems. Q_{in} = B_1 + B_2 - B_{CN}, with binding energies *B*'s taken from [7].

Finally, adding the Coulomb and centrifugal interactions to the nuclear interaction potential $V_N(R)$, we get the total interaction potential for deformed and oriented nuclei [8, 9], as

$$V_T^{\ell}(R, E_{c.m.}, \theta_i) = V_C(R, Z_i, \beta_{\lambda i}, T, \theta_i) + V_N(R, A_i, \beta_{\lambda i}, T, \theta_i) + V_{\ell}(R, A_i, \beta_{\lambda i}, T, \theta_i) \quad (15)$$

With V_{ℓ}, for non-sticking moment-of-inertia I_{NS} (= μR^2), given as

$$V_{\ell} = \frac{\hbar^2 \ell(\ell+1)}{2I_{NS}} \quad (16)$$

The Coulomb potential for a multipole-multipole interaction between two separated nuclei is given by

$$V_C(Z_i, \beta_{\lambda i}, \theta_i, T) = \frac{z_1 z_2 e^2}{R(T)} 3Z_1 Z_2 e^2 \sum_{i,i=1,2} \frac{R_i^{\lambda}(\alpha_i, T)}{(2\lambda+1)R(T)^{\lambda+1}} Y_{\lambda}^{(0)}(\theta_i)\left[\beta_{\lambda i} + \beta_{\lambda i}^2 Y_{\lambda}^{(0)}(\theta_i)\right] \quad (17)$$

Eq.(15) gives the ℓ-dependent barrier height V_B^ℓ, position R_B^ℓ, and the curvature $\hbar\omega_\ell$ for each ℓ, to be used in ℓ-summed extended-Wong model [8], discussed in the following section.

2.2 Extended ℓ-summed Wong Formula

According to Wong [10], the fusion cross-section, in terms of angular momentum ℓ partial waves, for two deformed and oriented nuclei, with orientation angle θ_i, colliding with the center-of-mass (c.m.) energy $E_{c.m.}$, is

$$\sigma(E_{c.m..},\theta_i)=\frac{\pi}{k^2}\sum_{\ell=0}^{\ell_{\max}}(2\ell+1)P_\ell(E_{c.m.},\theta_i) \tag{18}$$

With $k=\sqrt{\frac{2\mu E_{c.m.}}{\hbar^2}}$, and μ as reduced mass. Here, P_ℓ is the transmission coefficient for each ℓ which describes the penetration of the barrier i.e. $V_\ell(R, E_{c.m.}, \theta_i)$ and $\ell_{\max}$ is the maximum angular momentum.

Using Hill-Wheeler[11] approximation of finding the shape of the interaction barrier $V_\ell(R,E_{c.m.},\theta_i)$ through an inverted harmonic oscillator [$V_T^\ell(R,E_{c.m.},\theta_i) = V_B^\ell(E_{c.m.},\theta_i) - \frac{1}{2}\mu\omega^2(R - R_B^\ell)^2$], the penetrability P_ℓ in terms of its height $V^\ell_B(E_{c.m.},\theta_i)$ and curvature $\hbar\omega_\ell(E_{c.m.},\theta_i)$, is

$$P_\ell=\left[1+\exp\left(\frac{2\pi\left(V_B^\ell(E_{c.m.},\theta_i)-E_{c.m.}\right)}{\hbar\omega_\ell(E_{c.m.},\theta_i)}\right)\right]^{-1} \tag{19}$$

With $\hbar\omega_\ell(E_{c.m.},\theta_i)$, evaluated at barrier position $R=R_B^\ell$ corresponding to the maximum barrier height given as $V_B^\ell(E_{c.m.},\theta_i)$, given as

$$\hbar\omega_\ell(E_{c.m.},\theta_i)=\hbar\left[\left|d^2V^\ell(R)/dR^2\right|_{R=R_B^\ell/\mu}\right]^{1/2} \tag{20}$$

And, the R_B^ℓ obtained from the condition

$$\left| dV_T^{\ell}(R) \Big/ dR \right|_{R=R_B^{\ell}} = 0 \tag{21}$$

Noting that the ℓ-summed expression (20) uses the ℓ-dependent potentials [Eq.17]. Gupta and collaborators [8] carries out its ℓ-summation for $\ell_{\max}$ determined empirically for a best fit to measured cross-section, and the angles θ_i integrated to give the fusion cross-section

$$\sigma(E_{c.m..}) = \int_{\theta_i=0}^{\pi/2} \sigma(E_{c.m.}, \theta_i) \sin\theta_1 d\theta_1 \sin\theta_2 d\theta_2 \tag{22}$$

References:

[1] B. K. Agrawal, S. K. Dhiman, and R. Kumar, Phys. Rev. C 73, 034319(2006)

[2] M. Brack, C. Guet, and H. B. Hakansson, Phys. Rep. 123, 275(1985)

[3] J. Friedrich and P.G. Reinhard, Phys. Rev. C 33, 335(1986)

[4] A. Sandulescu, R. K. Gupta, W. Scheid and W. Greiner, Phys. Lett. 60B, 225(1976); Nucl. Phys. 9, 615(1959)

[5] R. K. Gupta, A. Sˇandulescu and W. Greiner, Phys. Lett. 67B, 257(1977); Rev. Roum. Phys. 23, 51(1978)

[6] G. Royer, J. Mignen, J. Phys. G: Nucl. Part. Phys. 18, 1781(1992)

[7] P. Moller, J. R. Nix et al., At. Nucl. Data Tables 59, 185(1995)

[8] R. Kumar, M. Bansal, S. K. Arun, R. K. Gupta, Phys. Rev. C 80, 034618(2009)

[9] R. K. Gupta et al., J. Phys. G: Nucl. Part. Phys. 31, 631(2005)

[10] C. Y. Wong, Phys. Rev. Lett. 31, 766 (1973)

[11] D. L. Hill and J. A. Wheeler, Phys. Rev. 89, 1102 (1953); T. D. Thomas, ibid. 116, 703 (1959)

Chapter 3

Outcomes and Discussions

Chapter 3

Role of Spin Saturated and Unsaturated Interaction Potentials in ^{23,25,27,29,31}Al + ^{45}Sc:

Here, we have investigated the isotopic dependence of interaction potential (both spin dependent and spin independent) using semiclassical extended Thomas-Fermi formulation in the framework of Skyrme Energy Density Functional theory using spherical and deformed choice of nuclei. This is done for isotopes of compound nucleus Se* formed by hitting variety of ^{23,25,27,29,31}Al projectiles on the fixed target ^{45}Sc.

The role of spin saturated interaction potential is shown to be important, as it contribute towards the total interaction potential and hence effects the fusion evaporation cross-sections [1]. In recent past, Gupta and collaborators [2, 3] studied the role of the spin-orbit density part of the interaction potential in Skyrme Energy Density Formalism (SEDF) and proposed a simple formulation of the potential for both the spin saturated and unsaturated interaction potentials. Different parameterizations i.e. different Skyrme forces of the interaction potential give different barrier characteristics.

In context of the fusion evaporation cross-section, we have used the ℓ-summed Wong Model [4] via the nuclear proximity potential obtained from the semiclassical extended Thomas-Fermi approach in SEDF under the frozen approximation and tested the recent data [5] of ^{27}Al + ^{45}Sc reaction.

Observations and Discussions:

Here we study the behavior of the spin-orbit density dependent potential $V_J(R)$ and spin independent part $V_P(R)$ for reactions ^{23,25,27,29,31}Al + ^{45}Sc with two choices i.e. spherical and deformation choice of interaction. The calculations are done by using semiclassical Extended Thomas-Fermi (ETF) approach in Skyrme Energy Density Formalism (SEDF) under frozen approximation.

Fig. 3.1 shows the spin-orbit density dependent interaction potential calculated by using semiclassical approach for isotopes of Se* formed using the projectile ^{23,25,27,29,31}Al on fixed target ^{45}Sc for spherical and deformed choice of nuclei at temperature $T = 0$.

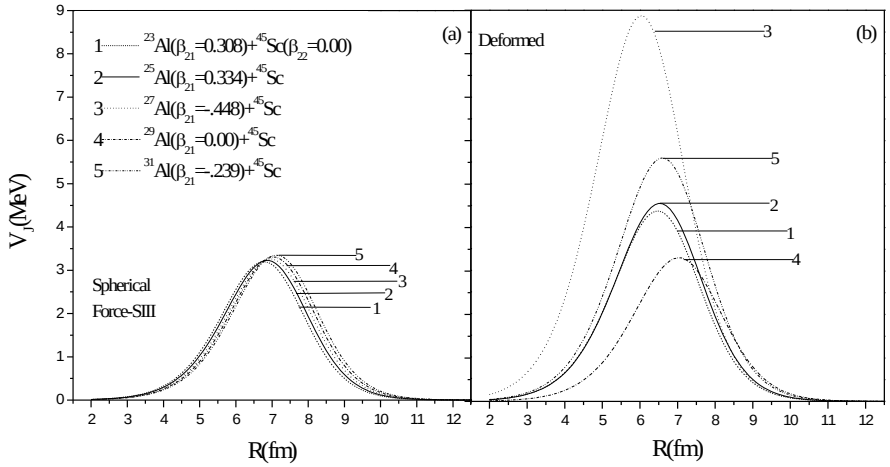

Figure 3.1 The comparison of spin dependent interaction potential for the isotopes of ^{27}Al forming compound nucleus ^{68,70,72,74,76}Se* using (a) spherical and (b) deformed choice of nuclei at $T = 0$ for force SIII.

It is observed from fig. 3.1 that the barrier height and barrier position increases systematically with addition of neutrons in projectile during spherical choice of interaction. As deformations are included with optimized orientations then barrier height changes but not according to the increase in the number of neutrons in the compound nucleus. In general the magnitude of spin dependent interaction potential increases in the inclusion of deformation effects, and particularly for oblate shape projectiles the magnitude enhancement is much steeper and barrier profile shifts towards the lower interaction radius. The results shown in the fig. 3.1 is only for Skyrme force SIII. In fig. 3.2 we have plotted the spin-orbit density dependent interaction potential V_J *(MeV)* for ^{27}Al + ^{45}Sc reaction for forces SIII and GSk1 [6] at temperature $T = 0$.

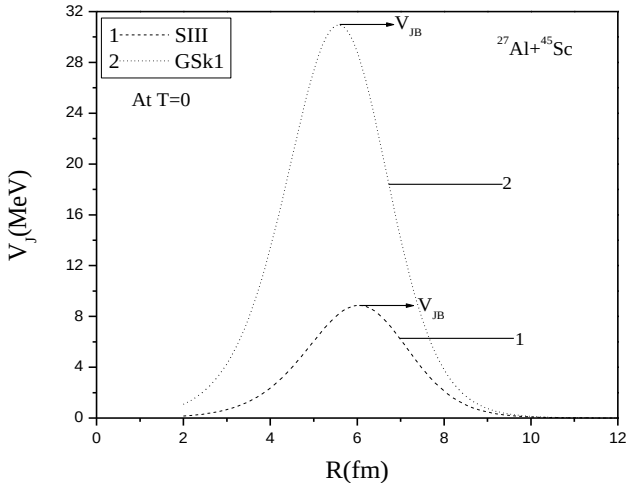

Figure 3.2 The Spin Dependent Potential V_J *(R)* at $T = 0$ of the system ^{27}Al + ^{45}Sc for two forces SIII and GSk1.

It has been observed from fig. 3.2 that the barrier height V_{JB} is more for GSk1 than SIII at $T = 0$. The possible reason for the increase in the height of barrier for force GSk1 could be associated in the extra parameters which are added in the third term (i.e. in density dependent term) of the Hamiltonian density and a new term that is added due to tensor coupling with spin and gradient. Details of this can be seen in [6]

The shift in the barrier position due to change in the number of neutrons and the deformations of the nuclei were discussed in fig 3.1. Following this, the difference in the barrier position for two different forces SIII and GSk1 is observed in fig. 3.2. One may note in fig. 3.2 that SIII force results in smaller barrier height V_{JB} and larger barrier position R_{JB}. Fig. 3.3 shows the total interaction potential V_T *(MeV)* again of the same system for two forces SIII and GSk1.

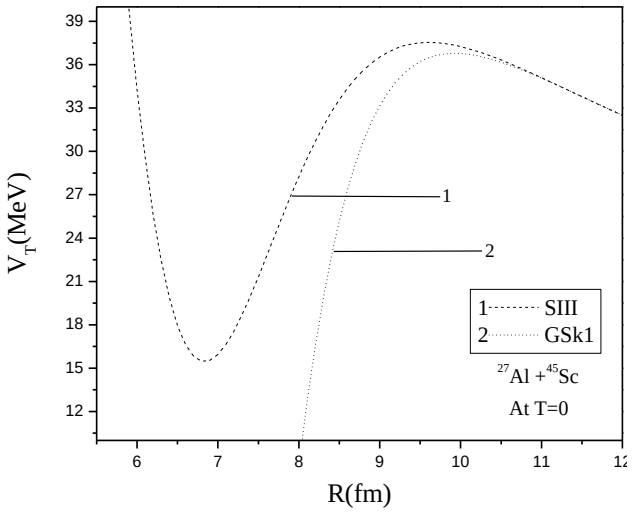

Figure 3.3 The Total Interaction Potential V_T *(MeV)* at $T = 0$ for ^{27}Al + ^{45}Sc reaction using forces SIII and GSk1.

It is well-known that the total interaction potential V_T *(MeV)* is the sum of the nuclear proximity potential which consists of spin-saturated and spin-unsaturated potential, and Coulomb interaction potential. Here we are interested to study the ground state properties of the interacting nuclei so we calculated the scattering potential at $\ell = 0$, but for calculating fusion excitation function, we include angular momentum potential as the interacting nuclei is in the excited state.

It may be noted from fig. 3.3 which shows the comparison of scattering potential for different Skyrme forces that barrier is highest for the SIII force and both the forces exhibit different barrier characteristics. Fig. 3.4 shows the effect of temperature on the spin-orbit density dependent interaction potential for the interacting isotopes of ^{27}Al on the fixed target ^{45}Sc using force SIII.

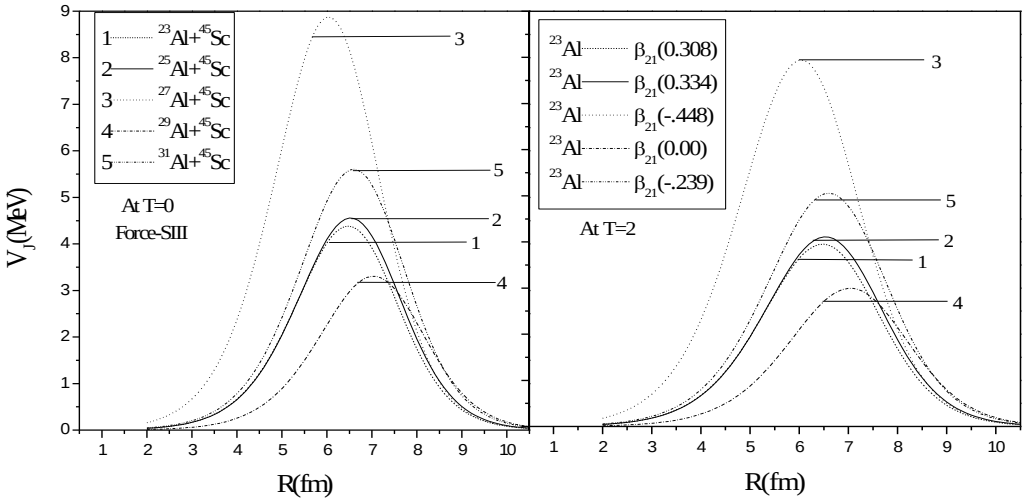

Figure 3.4 The Spin Dependent Interaction Potential V_J *(MeV)* of the isotopes of ^{27}Al forming compound nucleus ^{68,70,72,74,76}Se with β_2 deformation effects with in optimized orientations for force-SIII at T = 0, 2.

It is clearly observed from fig. 3.4 that the difference in the magnitudes of the barrier height of V_J (MeV) is decreased when going from temperature T = 0 to T = 2 for force SIII; the rest of the pattern remains same.

As we know that the spin-orbit density potential V_J *(MeV)* is repulsive in nature and spin-orbit density independent V_P *(MeV)* part is attractive in nature under frozen density approximation. So, V_J *(MeV)* part acts exactly opposite to the spin-independent part V_P *(MeV)* of the nucleus-nucleus potential. However, both of these terms are additive and essential to find the total interaction potential and further to investigate the fusion cross-sections. We have carried out the analysis of the spin-orbit density independent potential V_P *(MeV)* in the following fig. 3.5.

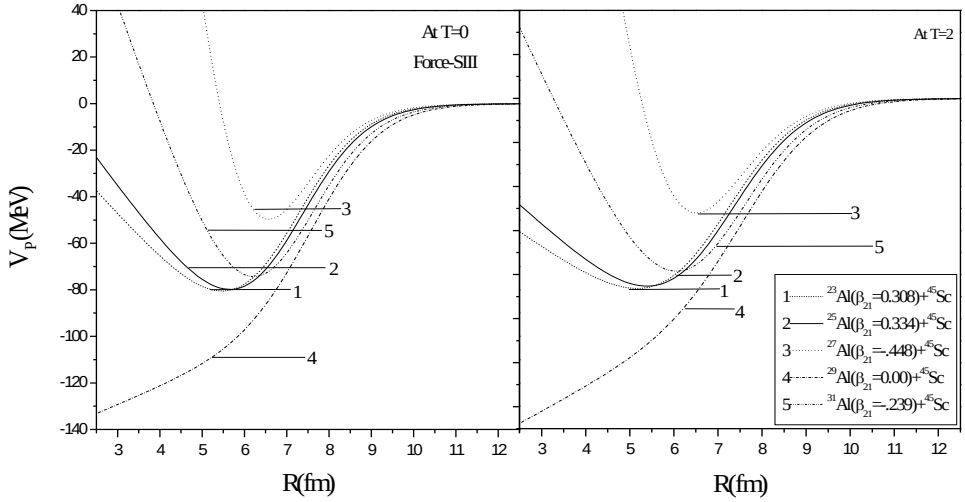

Figure 3.5 The Spin-independent interaction potential V_P *(MeV)* of the isotopes of Al forming compound nucleus ^{68,70,72,74,76}Se* with β_2 deformed choice values for force-SIII at T = 0, 2.

In fig. 3.5, it is shown that the spin-orbit density independent interaction potential V_P *(MeV)* shows the similar behavior for the isotopes of $^{72}Se^*$ compound nucleus formed using isotopes of Al bombarded on fixed target ^{45}Sc with the deformed and optimized orientations as we have seen for spin dependent potential V_J *(MeV)* in fig. 3.1. Also the temperature affects for the spin-independent potential is quite similar to that of the spin-dependent potential.

It is understood up to now that the changes due to the nuclear interaction potential affect the total interaction potential (as we discussed in the earlier fig. 3.3). And to know the behavior of the evaporation cross-section of the system, the total interaction potential V_T *(MeV)* plays an essential role in it. So the study of the behavior of total interaction potential V_T *(MeV)* of the isotopes of ^{27}Al forming the compound nucleus $^{68,70,72,74,76}Se^*$ including temperature i.e. T = 0, 2 is essential which is illustrated below in fig. 3.6.

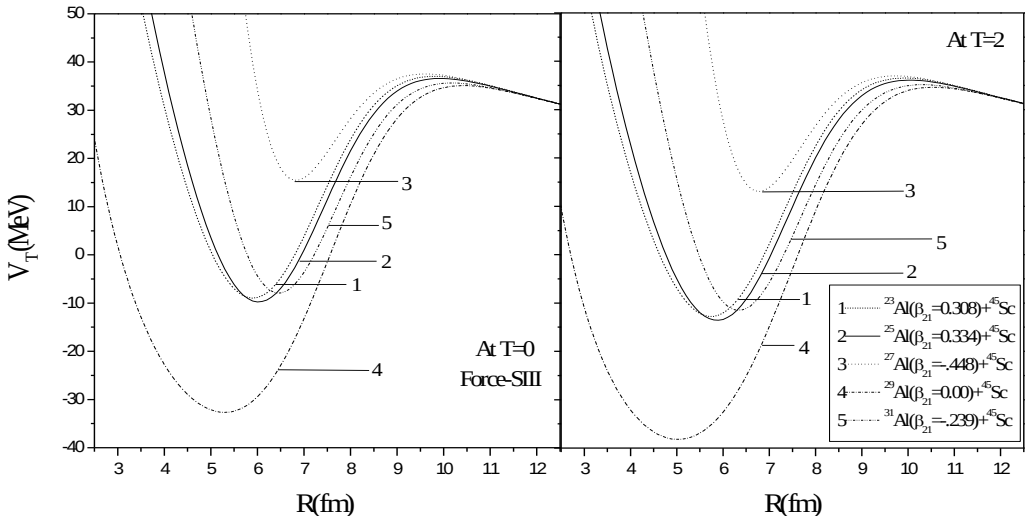

Figure 3.6 The total interaction potential V_T *(MeV)* of the isotopes of ^{27}Al forming compound nucleus $^{68,70,72,74,76}Se^*$ with deformed and optimized orientation values for force-SIII at T = 0, 2.

As we know, the barrier consists of the Coulomb and the nuclear potentials. However, the long range Coulomb repulsion between the nuclei is offset by stronger, but short range, attractive nuclear force. Then, the two nuclei are required to collide with sufficient kinetic energy to overcome their mutual electrostatic repulsion and subsequently to bring into effect the role of strong but short range attractive nuclear force. It means that the knowledge of interaction potential, forming barrier, between two nuclei is extremely important in order to have a systematic study of a nuclear reaction.

Fig. 3.6 gives the total interaction potential V_T *(MeV)* of the isotopes of Se^* compound nucleus at temperature T = 0, 2. The barrier of total interaction potential which is the sum of the barriers of the Coulomb interaction and nuclear proximity interaction exhibit the same trend for prolate and oblate deformations as seen for spin saturated and spin unsaturated interaction potentials.

Here, in our work, taking the advantage of the fact that, in ETF method, different Skyrme forces give different barriers (height, position and curvature) as shown on fig. 3.3, we use the ℓ-summed Wong model [8] under frozen density approximation for calculating the cross-sections.

Here, we calculated fusion evaporation cross-section in the framework of ℓ-summed Wong model using SEDF approach for ^{27}Al + ^{45}Sc system. Within ℓ-summed Wong model we find that the GSk1 and SIII forces fit the evaporation cross-section data almost exactly. The barrier characteristics (height, position, and curvature), which are extracted from the scattering potentials (in fig. 3.3), are the main inputs in the Wong model. The parameterizations of SIII force are less sensitive towards neutron-proton asymmetry and isospin effect so they provide an appropriate barrier characteristic, which fits the experimental data at the low barrier energies. Whereas the new GSk1 parameterization provides stronger isospin effect so the calculated fusion evaporation cross-section data is overestimated by this force GSk1 at lower energies.

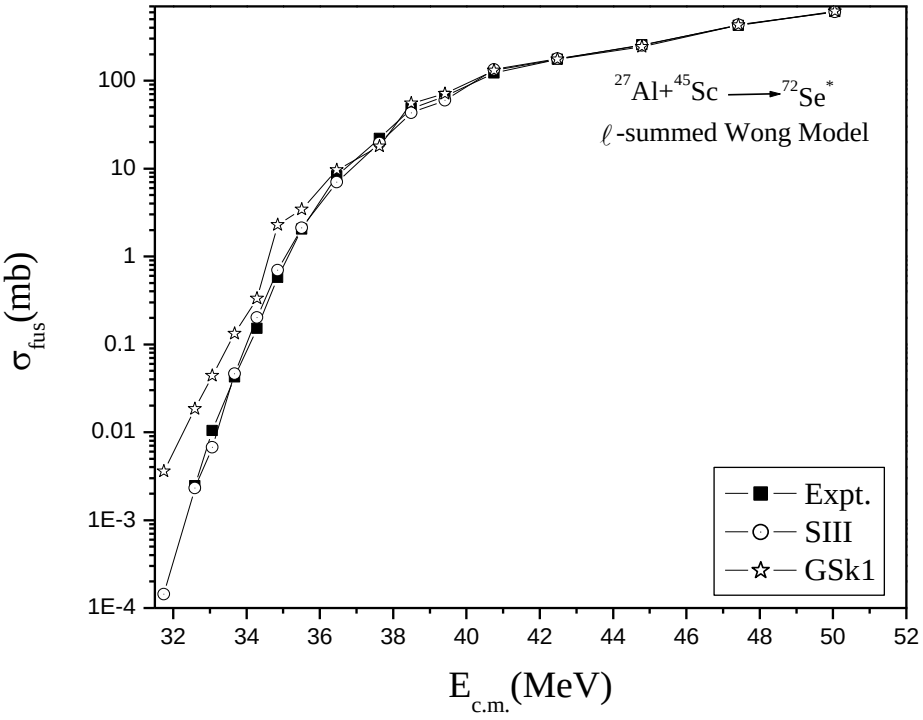

Figure 3.7 Fusion evaporation cross-sections of ^{27}Al + ^{45}Sc, calculated via the extended-Wong model for experimental data of $E_{c.m.}$ *(MeV),* using the Skyrme forces SIII and GSk1.

Apparently, the extended Wong model calculations for GSk1 and SIII forces fit the data nicely at both the above- and below-barrier energies, and hence no needs of barrier modification to be included in order to fit the data. The best possible fits of evaporation cross-sections with the two Skyrme forces i.e. GSk1 and SIII are shown in fig. 3.7. It is to be noted that at above as well as below the barrier, ℓ_{max} is almost same for both the forces as shown in table 3.1. The experimental

data were nicely expressed within ℓ-summed Wong Model for both forces with smooth variations of ℓ-values.

The analysis of fusion cross-sections of other isotopes investigated in this work is of future interest. Beside this one may also analyze for the role of higher order deformations in spin saturated and spin unsaturated interaction potentials for better understanding of chosen reaction.

Table 3.1 The Evaporation Residue cross-sections for ^{72}Se system, calculated by the ℓ-summed extended Wong-Model at different $E_{c.m.}$ *(MeV)*'s for two Skyrme forces i.e. SIII and GSk1, compared with the experimental data [5].

$E_{c.m.}$ (MeV)	Temperature (T)	Cross-Section (σ(mb))			ℓ_{max}	
		σ (Expt.)	σ (SIII)	σ (GSk1)	SIII	GSk1
31.74	0.9566	2.765637e(-4)	0.000143	0.00359	0	1
32.49	1.0075	0.00245342	0.002322	0.01839	1	1
33.06	1.0442	0.0104384	0.014384	0.04380	2	1
33.67	1.0825	0.0423719	0.04634	0.13273	2	1
34.28	1.1191	0.152083	0.20159	0.33165	2	1
34.85	1.1524	0.574221	0.696	0.61701	3	1
35.50	1.1890	2.03	2.11	3.42	3	3
36.46	1.2412	8.24	6.99	9.58	3	3
37.62	1.3013	21.93	19.41	17.92	4	4
38.48	1.3440	48.13	43.12	55.18	6	7
39.41	1.3884	65.98	59.90	71.11	7	8
40.75	1.4501	122.19	134.24	130.64	11	11
42.48	1.5259	175.70	178.71	174.99	13	13
44.78	1.6211	255.49	250.81	241.83	16	17
47.42	1.7234	424.86	433.10	428.93	22	22
50.05	1.8197	611.29	605.87	613.98	27	27

References:

[1] R. Kumar, M. Bansal, S. K. Arun, and R. K. Gupta, Phys. Rev. C 80, 034618 (2009).

[2] R. Kumar et al., Nucl. Phys. A 870-871, 42 (2011); R. Kumar and R. K. Gupta, J. Phys.: Conf. Ser. 312, 082025 (2011)

[3] R. K. Puri, R. Arora, and R. K. Gupta, Phys. Rev. C 60, 054619 (1999)

[4] C Y Wong, Phys. Rev. Lett. 31, 766 (1973)

[5] C. L. Jiang et al. Phys. Rev. C 81, 024611 (2010)

[6] B. K. Agrawal, S. K. Dhiman, and R. Kumar, Phys. Rev. C. 73, 034319 (2006)

[7] M. Dutra, O. Lourenco, and J. S. Sa Martins, Phy. Rev. C 85, 035201 (2012)

[8] R. Kumar, M. K. Sharma, and R. K. Gupta, Nucl. Phys. A 870, 42-57 (2011)